Critical phases of viral production processes monitored by capacitance

Emma Petiot, Sven Ansorge, Manuel Rosa-Calatrava, Amine Kamen

Journal of Biotechnology 242 (2017) 19–29

Contents lists available at ScienceDirect

Journal of Biotechnology

journal homepage: www.elsevier.com/locate/jbiotec

Critical phases of viral production processes monitored by capacitance

Emma Petiot[a,b,*], Sven Ansorge[a], Manuel Rosa-Calatrava[b], Amine Kamen[a,c]

[a] NRC, Human Health Therapeutics Portfolio, 6100 Royalmount Ave, Montréal, QC, H4P 2R2, Canada
[b] Virologie et Pathologie Humaine – VirPath Team, International Center for Infectious diseases Research, Inserm U1111, CNRS UMR5308, ENS Lyon, Université Claude Bernard Lyon 1, Faculté de Médecine RTH Laennec, Lyon, France
[c] McGill University, Bioengineering Dpt. 817, Sherbrooke St. W., Montreal, QC, H2 B 2C6, Canada

ARTICLE INFO

Article history:
Received 10 May 2016
Received in revised form 7 November 2016
Accepted 10 November 2016
Available online 17 November 2016

Keywords:
On-line monitoring
Capacitance probe
Permittivity
Characteristic frequency fc
Virus production kinetics
Dielectric cell properties
Membrane capacitance
Viral infection

ABSTRACT

Over the last decade industrial manufacturing of viral vaccines and viral vectors for prophylactic and therapeutic applications is experiencing a remarkable growth. Currently, the quality attributes of viral derived products are assessed only at the end-point of the production process, essentially because in-process monitoring tools are not available or not implemented at industrial scale. However, to demonstrate process reproducibility and robustness, manufacturers are strongly advised by regulatory agencies to adopt more on-line process monitoring and control. Dielectric spectroscopy has been successfully used as an excellent indicator of the cell culture state in mammalian and yeast cell systems. We previously reported the use of this technique for monitoring influenza and lentiviral productions in HEK293 cell cultures. For both viruses, multi-frequency capacitance measurements allowed not only the on-line monitoring of the production kinetics, but also the identification of the viral release time from the cells. The present study demonstrates that the same approach can be successfully exploited for the on-line monitoring of different enveloped and non-enveloped virus production kinetics in cell culture processes. The on-line monitoring multi-frequency capacitance method was assessed in human HEK293 and Sf9 insect cells expression systems, with viral productions initiated by either infection or transfection. The comparative analyses of all the data acquired indicate that the characteristic capacitance signals were highly correlated with the occurrence of viral replication phases. Furthermore the evolution of the cell dielectric properties (intracellular conductivity and membrane capacitance) were indicative of each main replication steps. In conclusion, multi-frequency capacitance has a great potential for on-line monitoring, supervision and control of viral vector production in cell culture processes.

1. Introduction

In recent years, an increasing number of viral products have been evaluated and approved, either for vaccination or therapeutic approaches, and numerous vectors and viruses are currently evaluated in preclinical and clinical research programs (Brun et al., 2008; Buonagurio et al., 2006; Draper and Heeney, 2010; Haupt and Sings, 2011; Lentz et al., 2011; Van Gessel et al., 2011). Virus production is a broad and highly diverse field, comprising different virus types, production methods and the use of various cellular platforms (Ansorge et al., 2009; Aucoin et al., 2007; Durocher et al., 2007; Ghani et al., 2006; Kamen and Henry, 2004; Knop and Harrell, 2007; Le Ru et al., 2010; Meghrous et al., 2005; Paillet et al., 2009; Pau et al., 2001; Petiot et al., 2012b; Whitford and Fairbank, 2011; Wong et al., 1994). Manufacturing processes require high levels of compliance and quality control. Consequently, guidelines from the regulatory agencies recommend to systematically monitor the "quality" of such productions, not only as an end-point control, but also through implementation of continuous in-process analytical and monitoring technologies. It will allow to document the process and assess its robustness and reproducibility. The goal of this approach is ultimately to i) in-line monitor the accumulation of bioactive viral particles in the cell culture, ii) enable quality-by-design of the process by ensuring in real-time product quality, process consistency and reproducibility (FDA, 2004).

In general, on-line monitoring of the accumulation of the bioactive viral particles in cell culture remains for the moment out of reach due to the fact that non-invasive methods have not been developed to achieve this goal. However, monitoring and super-

* Corresponding author at: Université Claude Bernard Lyon 1, Laboratoire VirPath, CIRI Inserm CNRS U1111, Faculté de médecine RTH Laennec, 7 rue Guillaume Paradin 69008 Lyon, France.
E-mail addresses: emma.petiot@univ-lyon1.fr (E. Petiot), sven.ansorge@cnrc-nrc.gc.ca (S. Ansorge), manuel.rosa-calatrava@univ-lyon1.frm (M. Rosa-Calatrava), amine.kamen@mcgill.ca (A. Kamen).

http://dx.doi.org/10.1016/j.jbiotec.2016.11.010
0168-1656/

vision of key process parameter trends are feasible when using state-of-the-art techniques. To do so, we propose to focus on methods measuring the morphological and physiological alterations of the cell population that occur during each step of the viral replication cycle (cellular entry, replication, genome assembly, budding and/or cell lysis). Many events are associated with the cell infection process and the viral replication cycle. The physiology and morphology of the infected cells are significantly affected. The viral hijacking of cellular machineries and associated remodeling of their ultrastructure and compartments lead to strong modifications of the cellular and the cell populations 'fingerprints' (Josset et al., 2008; Terrier et al., 2012). During the viral production cycles, the intracellular content, the membrane protein composition as well as its integrity are very likely to change. For example, Sf9 cell size increases during baculovirus productions (Palomares et al., 2001), influenza and HIV viral infections induce cell apoptosis (Al-Rubeai and Singh, 1998; Hinshaw et al., 1994) and cytolytic viruses are responsible for modifications of the cell membrane permeability (Costin, 2007). Therefore, the biomass (a function of cell size and number) and the physiological characteristics of the cultivated cells are primary indicators of the progress of viral infection and progeny viral particle production.

Capacitance is probably one of the best and most advanced techniques for the on-line monitoring of cell biomass and physiological state and has been extensively described over the past 20 years (Ansorge et al., 2007; Ansorge et al., 2010b; Elias et al., 2000; Opel et al., 2010; Zeiser et al., 1999) It measures the cell biovolume and has been shown to respond to changes in a number of cellular properties. Its principle is based on the theory of Schwan where cells are considered as small capacitors. The models describing cell capacitance behaviour under polarization at different frequencies link dielectric constants (the permittivity ($\Delta\varepsilon_{max}$) and the characteristic frequency (fc)) to the physiological characteristics of cultivated cells and their biomass (the intracellular conductivity (σi), the membrane capacitance (Cm), the cell biovolume (Bv), and the cell size (r)). This technology has already been assessed and successfully used to monitor growth and death for a number of different cell lines (Ansorge et al., 2010a,b, 2007a,b; Ansorge et al., 2007; Ducommun et al., 2002; Noll and Biselli, 1998; Opel et al., 2010; Párta et al., 2013; Petiot et al., 2012a; Zalai et al., 2015; Zeiser et al., 1999). In addition, the potential to use $\Delta\varepsilon_{max}$ or fc signals to monitor the viral production process evolution has been established (Ansorge et al., 2011; Petiot et al., 2012b).

In parallel, complementary off-line methods, such as electrorotation and dielectrophoresis, have been used to assess correlations between cell dielectric properties (σi, Cm) and specific biological characteristics (Arnold and Zimmermann, 1988). These include cell membrane thickness and folding which both impact the Cm value (Archer et al., 1999; Genet et al., 2000; Zimmermann et al., 2008). Furthermore, the two dielectric parameters, membrane capacitance (Cm) and intracellular conductivity (σ_i), can be inferred from the incremental values of permittivity ($\Delta\varepsilon_{max}$), characteristic frequency (fc), medium conductivity (σ_m) and cell size (r) using Schwan model (see equations 3 & 4). Also, Cm and σi have been used to study the impact of cell death on macroscopic signals (Opel et al., 2010; Tibayrenc et al., 2011), and intracellular conductivity was recently identified as an indicator of the cell physiological state in cell culture process (Ansorge et al., 2010b).

In the present study, the on-line capacitance data from different viral production systems (virus type, cell-lines, production mode) were extensively analyzed. Three enveloped viruses (lentivirus, influenza virus, baculovirus) and one non-enveloped virus (reovirus) were produced on two cellular platforms, HEK293 cells and Sf9 cells. All the viruses were produced by direct infection with the exception of lentivirus that was generated from a co-transfection of four plasmids. The selected viruses were different in many aspects, including the localization of viral replication (nucleus vs cytoplasm) and assembly (cytoplasm vs cell membrane), the mode of viral release (budding vs lysis) and the viral l morphology (spherical vs rod-shape) which broadened the scope of the study and allowed to propose general conclusions. Moreover, two different multiplicities of infection (MOI) were used in baculovirus productions to evaluate the impact of viral production kinetics on the capacitance monitoring signals. Signal trends were correlated with biological events occurring during the viral replication process. These biological events were directly correlated with cell dielectric parameters profiles (r, Cm and σi) focusing on three key phases for any viral production i) intracellular accumulation of viral components and viral assembly (**Phase I**), ii) viral release (**Phase II**) and iii) cell death (**Phase III**). Overall the results of this work demonstrate that dielectric spectroscopy is a convenient and generic on-line method to detect phases and progression of viral productions.

2. Material & methods

2.1. Viral productions

Different viruses and modes of production were selected for their variable effects on cellular morphology and cell dielectric properties during the course of viral replication. Typical virus production runs were monitored using an on-line capacitance probe and one non-enveloped and three enveloped virus productions were analyzed in detail. To do so, we focused on the analysis of infectious viral particles which we are considered as having completed their viral life cycle.

On-line measurements from the capacitance probe acquired the dielectric parameters of the cultures as described in the M&M Section 3. The descriptions of the bioreactor set-up and feeding strategy have been already presented in detail in the associated published work for lentivirus (Ansorge et al., 2011), influenza virus (Petiot et al., 2011) and baculovirus (Bernal et al., 2009). The cultures presented herein for influenza and lentivirus productions were also part of these articles, describing either viral production process development and/or production kinetics. Both Reovirus and Baculovirus cultures are original work that was not previously published, but for baculovirus viral production kinetics (cell density, cell viability, viral titers) were comparable with previous work published by the group on baculovirus production processes (Elias et al., 2000). Critical information necessary for the understanding of the present work is provided in the following section and Table 1.

2.1.1. Non-enveloped virus production: reovirus production

Reovirus production in HEK 293 cells was selected to represent a non-enveloped viral production process. Productions were performed in batch mode including a dilution of the culture prior to infection. Cultures were inoculated at cell density of 0.4×10^6 cell/mL in I.A. 65719 medium (SAFC) supplemented with 4 mM glutamine. The dilution-step was performed immediately before infection after 2 days of culture once a cell density of $1.8 - 2.4 \times 10^6$ cell/mL was reached. The bioreactor system used was a Chemap 3.5 L (working volume 2.8–3 L), previously described in Le Ru et al. (2010), but with minor modifications.

2.1.2. Enveloped virus productions

2.1.2.1. Influenza virus production. Influenza virus was produced in a 3.5-L Chemap bioreactor with a 2.9 L working volume. The bioreactor set-up has been already well described elsewhere (Le Ru et al., 2010). Cells were seeded at 0.25×10^6 cell/mL and were infected when the culture reached 6×10^6 cell/m. Infection of culture is performed at a MOI of 0.01 with the preliminary addition of TPCK-Trypsin (Sigma) at a final concentration of 1 μg/mL. Progeny

Table 1
Summary of the viral production process monitored on-line by multi-frequency capacitance probe.

	Virus	Family	Mean Size	Cell Line	Production process	Multiplicity of Infection (MOI)
Non-enveloped virus	Reovirus	Reoviridae	80 nm	HEK293 S human	infection	0.5
Enveloped virus	Influenza	Orthomyxovirus	100 nm	HEK293 SF human	Infection	0.01
	Lentivirus	Retrovirus	100 nm	HEK293 SF human	Transfection 4 plasmids	n/A
	Baculovirus	Baculoviridae	300 nm length (rod shaped)	Sf9 insect	Infection	0.2 & 2.0

infectious influenza virus were titered from culture supernatant collected during the production process. The titration method was a TCID50 assay performed on MDCK confluent cells already described in the related paper (Petiot et al., 2012b, 2011).

2.1.2.2. Lentivirus production. Lentivirus production was performed using PEI-mediated co-transfection of four plasmids encoding for the viral proteins and genome. All productions were performed in 3.5 L Chemap bioreactor perfusion cultures and transfections were done once a cell density of 5.8×10^6 cell/mL was reached. To increase expression of the lentiviral vector components, 5 mM sodium butyrate was added to the culture 16 h post-transfection (Ansorge et al. 2009; Ansorge et al., 2010b). infectious lentivirus particles were quantified by a cytometry technique titled gene transfer assay (GTA) developed and described in Ansorge et al. (2011) (Segura et al., 2006). This method allows for quantification of the functional viral particles through measurement of the number of transduced GFP-expressing cells.

2.1.2.3. Baculovirus production. Baculovirus productions were performed in 3.5 L Chemap bioreactor using Sf9 cell cultures. Sf9 cells were seeded at 0.5×10^6 cell/mL in Sf900™ II SFM medium (Invitrogen). Infection of cultures was done at a cell density of 3×10^6 cell/mL. Baculovirus stocks used for these productions were produced in-house with the BD Bioscience baculogold system and pVL1393 vector backbone. Two different constructions were produced, containing either neuraminidase or hemagglutinin influenza genes. They were respectively named NA-BV and HA-BV. Two different MOI were used for these baculovirus productions, 0.2 for NA-BV and 2.0 for HA-BV. Bioreactors were controlled at 40% dissolved oxygen and at a temperature of 25 °C. Infectious baculovirus TCID50 titration were performed using Easy titer technique with Sf9 cells expressing GFP when infected (Hopkins and Esposito, 2009).

2.2. Cell size measurement

Mean cell diameter (d = 2 x r) was measured using a Z2TM Coulter Counter® (Beckman Coulter, Mississauga, ON) with an aperture diameter of 100 μm. Analysis of the size distributions was then performed with the associated Accucomp® software package (Beckman Coulter). In the case of HEK293 cell cultures, cellular aggregates could affect the measurement. Consequently, cell aggregates were described by Côté et al. (1998). This step was not necessary in the case of Sf9 cells.

2.3. On-line multi-frequency permittivity monitoring and data treatment

Cultures were monitored in real-time with the Fogale Biomass System® (scanning module and software Biomass 400®) (Fogale Nanotech, Hamilton Bonaduz AG, Nîmes, France). Permittivitiy was acquired at frequencies ranging from 0.1 to 10 MHz every 6 min. From the raw data, the Biomass 400® software provides the β-dispersion parameters (Maximum permittivity $\Delta\varepsilon_{max}$, characteristic frequency, fc) (Ansorge et al., 2007; Ansorge et al., 2010a; Opel et al., 2010). In addition to β-dispersion parameters, the medium conductivity (σ_m) is also monitored on-line by the Biomass System.

The mathematical model of Pauly and Schwan (Pauly and Packer, 1960; Schwan, 1957) describes the β-dispersion as the polarization of spherical vesicles. In this model, the maximum amplitude in permittivity $\Delta\varepsilon_{max}$ and fc are dependent on physical or biological cell properties. Both of these parameters are described by the model as functions of the following variables: the cell biovolume (Bv), the cellular membrane capacitance (Cm), the cell radius (r), the intracellular conductivity (σi) and the medium conductivity (σm) (Eqs. (1) & (2)). Consequently, the dielectric parameters, Cm and σi, can be derived from the values of $\Delta\varepsilon_{max}$, σm, fc, r and Bv as described by Eqs. (3) & (4).

On-line data processing was performed by averaging the on-line measurements of $\Delta\varepsilon_{max}$, σm and fc over a period of 0.5 h. Biovolume (Bv) was calculated from off-line measurements of cell diameter (2 x r) (Section 2.2) and total cell concentrations over time. Bv was derived from these measurements as the volume fraction of viable cells in the cell culture volume. All the data ($\Delta\varepsilon_{max}$, σm, fc, d: 2 x r, Bv) were smoothed with Kyplot software (KyensLab Inc.) with a spline regression. Spline curves were then incremented to one point per hour and dielectric parameters Cm and σi, were calculated according to Eqs. (3) & (4). The differences between these treated data points and the actual values allowed evaluating the RMSE (root mean square error), corresponding to signal noise in the case of fc, $\Delta\varepsilon_{max.}$ and σ_m. The RMSE errors allowed to evaluate the error propagated to the Cm and σi calculation, and to determine a significance cut-off for their evolution. The RMSE propagated errors calculated for Cm and σi were respectively 0.69%, and 2%. The changes in dielectric parameters were thus considered as significant for changes above 2% (see Table 2).

$$\Delta\varepsilon_{max} = 3\pi \times r^4 \times N \times Cm \quad (1)$$

$$fc = \frac{1}{2\pi \times r \times Cm \times ((1 \div \sigma i) + (1 \div 2\sigma m))} \quad (2)$$

$$\sigma i = \frac{8\pi \times fc \times \Delta\varepsilon max \times \sigma m}{9 \times Bv \times \sigma m - 4\pi \times fc \times \Delta\varepsilon max} \quad (3)$$

$$Cm = \frac{4 \times \Delta\varepsilon max}{9 \times r \times Bv} \quad (4)$$

$\Delta\varepsilon_{max}$: permittivity (pF m^{-1})
r: cell radius
Cm: cell membrane capacitance (F m^{-2})
Bv: volume fraction of cells in the culture medium (%)
N: Cell concentration (cell/mL)
fc: characteristic frequency (kHz)
σi: intracellular conductivity (mS Cm^{-1})
σm: medium conductivity (mS Cm^{-1})

Remark: Each of these calculated parameters is representative of the entire cell population (or the average) at the time of the measurement in the bioreactor, and it is not possible to discriminate

Table 2
Significance of dielectric parameters evolutions: |x| represents the percentage of evolution of a parameter (P) calculated per hour as follows: $((P_{t+1}-P_{t-1})\times 100)\div((t+1)-(t-1)\times P_t)$.

Dielectric parameter evolution/hour, (|x|)	0% ≤ |x| ≤ 2%	2% ≤ |x| ≤ 5%	|x| ≥ 5%
Significance (Symbol)	No evolution (∼)	Significant increase (↑) or decrease (↓)	High increase (↑↑) or decrease (↓↓)

between the different sub-populations (i.e. infected/non-infected; live/dead).

2.4. Membrane size evaluation by electron microscopy

Shake flask cell cultures of HEK293 cells were grown to a density of 2×10^6 cell/mL (120 rpm, 37 °C, 5% CO_2) and infected with influenza A/Puerto Rico/8/34 H1N1 strain at a MOI of 0.01 (trypsin concentration of 1 μg/mL). Cell growth and death was monitored for 3 days to evaluate the consistency with bioreactor experiments. A mock culture of HEK293 cells was grown in parallel and sampled at the same time. Cell culture samples of 2 mL were fixed with 2% Glutaraldehyde. The samples were washed three times in saccharose 0.4 M/0.2 M Na C-HCl-Cacodylate-HCl pH 7.4 (1 h at 4 °C) and post-fixed with 2% OsO4/0.3 M Na C-HCl-Cacodylate-HCl pH 7.4 (1 h at 4 °C). Then, cells were dehydrated with an increasing ethanol gradient (5 min in 30%, 50%, 70%, 95%, and 3 times for 10 min in absolute ethanol). Impregnation was performed with 50% Epon A, 50% Epon B and 1.7% DMP30. Inclusion was obtained by polymerization at 60 °C for 72 h.

Ultrathin sections (approximately 70 nm thick) were cut on a Reichert ultracut E (Leica) ultramicrotome, mounted on 200 mesh copper grids coated with 1:1000 polylisine, and stabilized for 1 day at room temperature (RT) and, contrasted with uranyl acetate and lead citrate. Sections were examined with a Jeol 1400JEM (Tokyo, Japan) transmission electron microscope equipped with an Orius 600 camera and Digital Micrograph.

3. Results and discussion

3.1. Non-enveloped viruses

In order to observe effects of viral production kinetics on permittivity on-line signals, $\Delta\varepsilon_{max}$ and fc values were plotted against data generated with off-line analyses. Biovolume, cell concentration, cell size, cell viability and infectious viral titers analyzed from the culture supernatant or the total broth (including intracellular virions) are presented in Fig. 1. The medium conductivity, σm, was monitored as an indicator of cell environment evolution (base addition, toxic compound released as metabolic by-products, osmolality) as it could impact fc parameters. Its variation during the viral production was considered as non-significant to explain the following dielectric parameters evolutions as Δσm was of 1.6 mS/Cm (eq. to 10% of σm mean values). We should indicate that the increase happens from the onset of cell death, after 20 hpi, and is concomitant with base addition.

According to the theory of Schwan, the permittivity of a cell culture is directly correlated to the cell biovolume and cell concentration. In the present case, the on-line acquisition of the $\Delta\varepsilon_{max}$ signal allowed supervising different process steps. At the beginning of the culture, the permittivity signal showed a similar trend than cell concentration and biovolume (Fig. 1-A). The growth phase before and after infection was characterized by a permittivity and biovolume increase. This phase lasted for approximately 35 h post-infection. When the cell death phase started at 35 hpi when viability dropped below 90% a concomitant decrease in permittivity values was observed. The dilution step, reducing the viable cell density

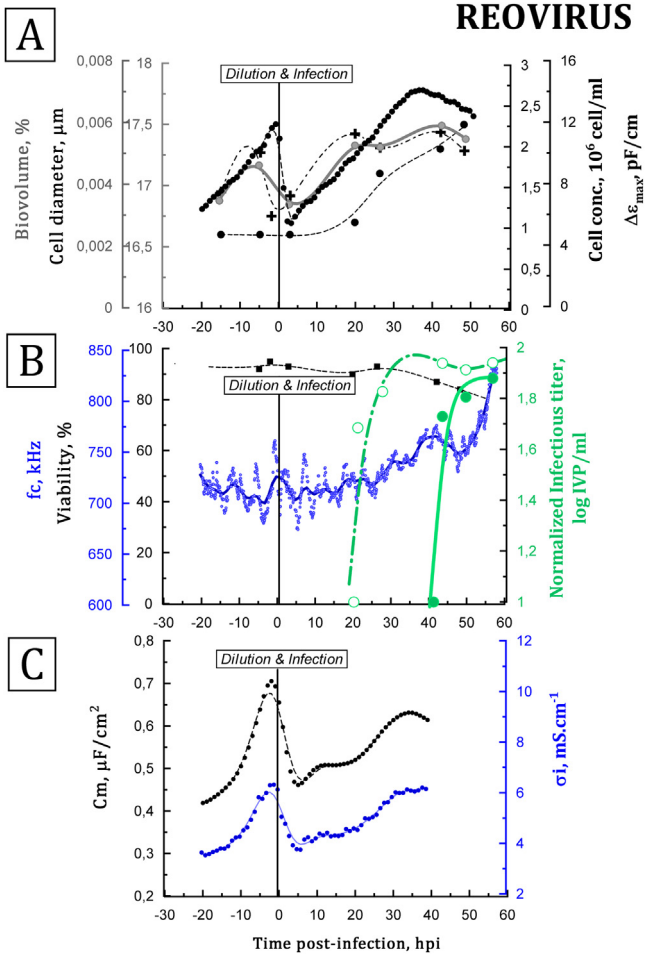

Fig. 1. Monitoring of reovirus production. A- Biovolume (●), Cell size (- -●- -), Cell concentration (+) and permittivity signal (●●●) B- Cell viability (-■-), Released infectious viral particles (●), Total infectious viral particles (⊖) = intracellular and released particles, and fc signal (–●–). C- Intracellular conductivity σi (●●●) and membrane capacitance Cm (●●●).

Table 3
Dielectric parameters evolutions for non-enveloped virus (reovirus): Viral production kinetic events referred to dielectric calculated (Cm, σi) and morphologic (r) measured parameters. On-line signal evolutions are also presented; arrows up indicate a significant increase, arrows down a significant decrease of the parameters. Significance of the evolution was set as described in Material and Method section according to error calculation presented in Table 2.

Production Phase	Significant On-line signals evolution		Viral kinetic	Dielectric Parameter evolutions
I (5–40 hpi)	fc∼	Δε↑	Intracellular accumulation of viral particles	σi ↑ – Cm ↑ – r ↑
II & III (40–50 hpi)	fc ↑	Δε↓	Start of cell death – Release of viral particles	r≅

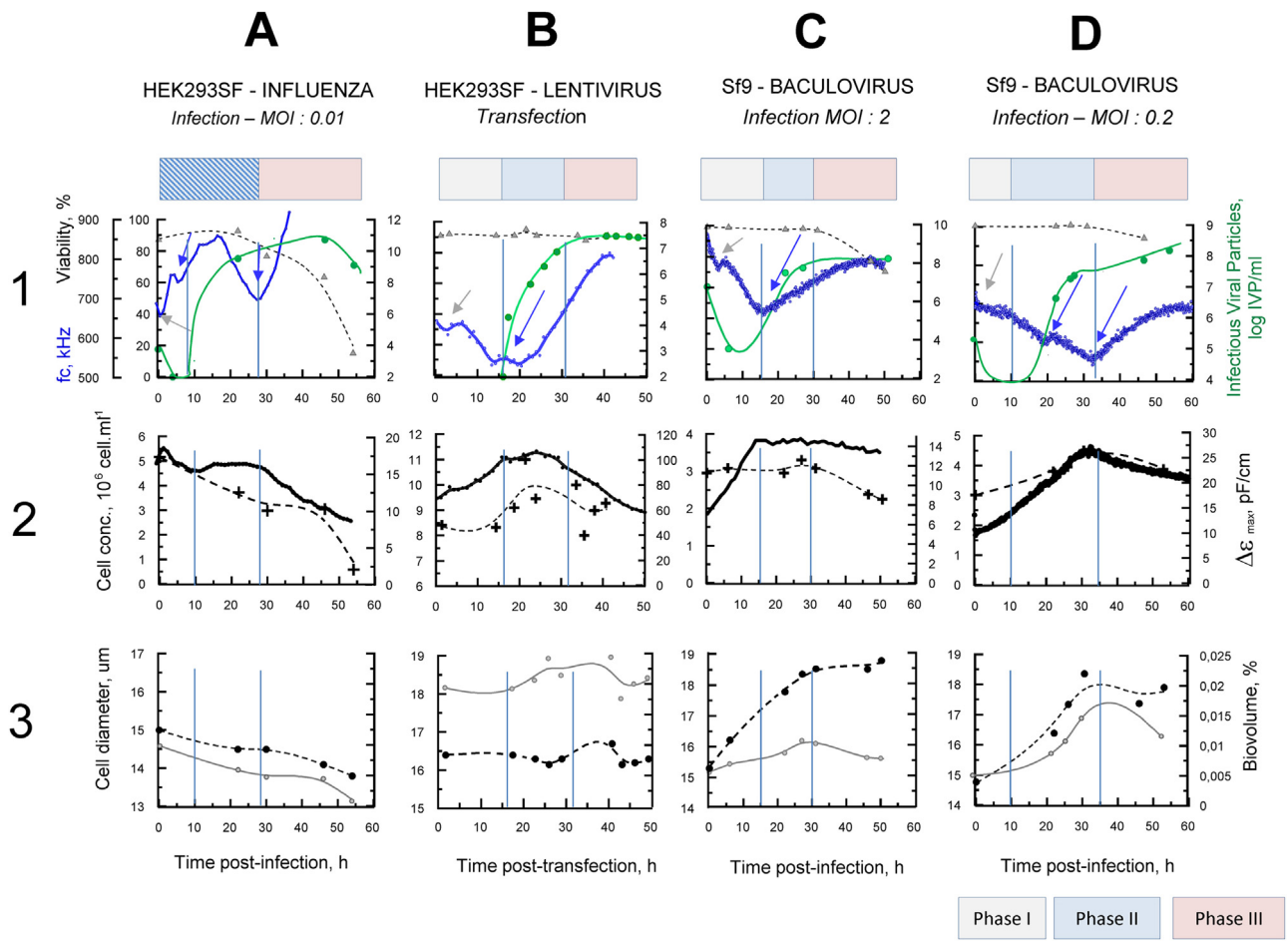

Fig. 2. Monitoring of the different production process of enveloped viruses: Influenza/Lentivirus/Baculovirus MOI 2.0/Bacculovirus MOI 0.2. First row- fc (–●–), Infectious viral particles (●), viability (—.—). Second row- Cell viable concentration (+), Permittivity (●). Third row-: Cell size (–●–), Biovolume (●).

immediately before infection by half, is also clearly visible as a drop in the permittivity signal (Fig. 1-A).

Physical or physiological changes of a cell culture during viral replication are expected to have an impact on cell size and cell biovolume. Such observations have already been reported for various cell lines (CHO, Sf9) and production modes (Batch – Fed-batch – Perfusion) (Ansorge et al., 2010a,b, 2007). For non-enveloped virus types, cell size is a good indicator of the viral production stage as already reported for adenovirus using capacitance monitoring (Ansorge et al., 2010c,d). Here, we observed an increase up to 17.5 nm of cell diameter after infection, caused most likely by the accumulation of cytoplasmic viral materials and numerous assembled viruses inside the nucleus.

The fc profile is more complex to analyze due to its high variability during the first phase of the culture (oscillation between 700 and 750 kHz) at the low cell densities of 1–2 million cell/mL. Clear changes in fc were however observed when cell death was initiated by viral release, an event that is often accompanied by the onset of apoptosis and cell shrinkage. At 35 hpi, when HEK293 cells started dying, fc values increased drastically. Such phenomena have already been described for different microbial and mammalian cell systems, with and without viral production (Opel et al., 2010; Petiot et al., 2012a; Tibayrenc et al., 2011). For adenovirus production similar fc and $\Delta\varepsilon_{max}$ patterns and production kinetics were obtained by the authors (data not shown).

3.1.1. *Viral cycle and production kinetics*

As indicated in the introductory section, three phases of the viral replication process could be identified from growth and viral kinetics. For the reovirus production kinetics, progeny virions were detected intracellularly as early as 19 hpi, but were detected in the culture supernatant only at cell death onset (after 35 hpi). This observation implies that a first phase (**Phase I**) corresponding to viral component synthesis and assembly of progeny viruses, lasted until 35 hpi. The second phase (**Phase II**) corresponds to the viral release, and the third phase (**Phase III**) to the induced cell death. Progeny virions for naked virus are commonly released by cell lysis, meaning that in the case of reovirus production both **Phase II and III** start at 35 hpi. Calculation of the two dielectric parameters, membrane capacitance Cm and intracellular conductivity σi allowed for an in-depth analysis of the capacitance signals and to compare and link their evolutions with known biological events (Fig. 1-C & Table 3).

Values obtained for Cm and σi are consistent with values found in the literature. Cm varies between 0.4 and 0.7 $\mu F\,Cm^{-2}$, where it is generally reported close to 1.0 $\mu F\,Cm^{-2}$ for HEK293 cells (Labeed et al., 2006; Zimmermann et al., 2008, 2006). As for measures of intracellular conductivities, values reported for cardiac cell tissue are of 1.5 to 5 $mS\,Cm^{-1}$ (Bronzino and Roth, 2000; Stinstra et al., 2005); and the ones for human chronic myelogenous leukaemia (K562) cells, used for apoptosis study, have a σi ranging from 2.7 to

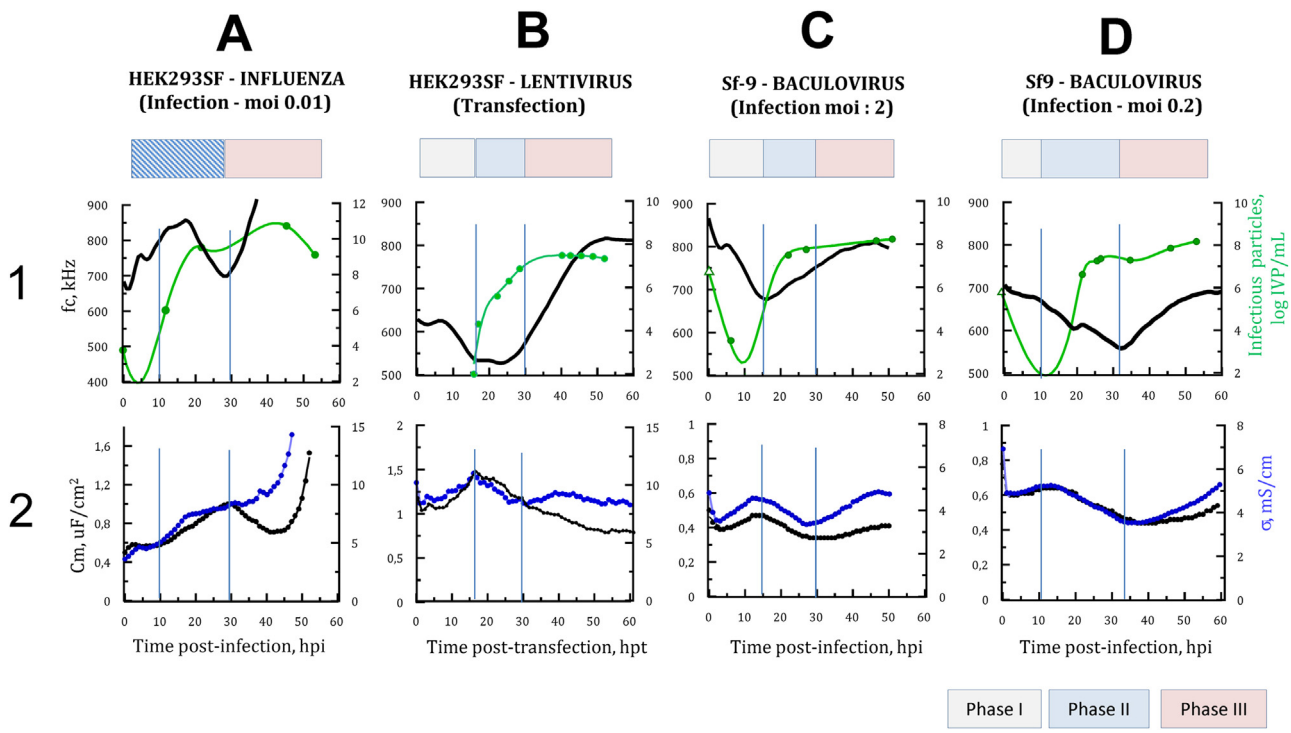

Fig. 3. Evolution of intracellular conductivity (σi) and membrane capacitance (Cm) for enveloped virus productions: fc (–), viral titers (●), Cm (●), δi (●). For baculovirus productions, open triangle symbol (Δ) indicate theoretical IVP present at time of infection based on the IVP injected in the bioreactor cultures.

Table 4
Summary of the membrane capacitance, Cm, and intracellular conductivity, σi, evolutions during the production processes of enveloped viruses. Arrows up indicate an increase, arrows down a decrease of the parameters. Significance of the evolution was set as described in Material and Method section according to error calculation (see Table 2).

Production Phase	Viral kinetic	On-line signals & dielectric parameters evolutions			
		Influenza virus MOI 0.01	Lentivirus	Baculovirus MOI 2	Baculovirus MOI 0.2
I	Intracellular accumulation of viral protein & Membrane folding	σi ↑/Cm ↑ (1–30 hpi)	σi ↑/Cm ↑ (2–17 hpi)	σi ↑/Cm ↑ (2–15 hpi)	σi ↑/Cm ↑ (2–10 hpi)
II	Massive Viral Release	σi ~ /Cm ↑ (15–30 hpi)	σi ↓/Cm ↓ (17–30 hpi)	σi ↓/Cm ↓ (15–30 hpi)	σi ↓/Cm ↓ (10–35 hpi)
III	Cell death	fc ↑↑ – Δε ↓ (30 to –60 hpi)	fc↑- Δε ↓ (30–45 hpi)	fc↑- Δε ↓ (30–50 hpi)	fc↑- Δε ↓ (35–60 hpi)

3.2 mS Cm^{-1} (Labeed et al., 2006). In the present case, σi of infected HEK293 cells is in the range of 4 to 6 mS Cm^{-1}

During **Phase I** (from 5 hpi to 35 hpi), Cm and σi increased by more than 25% over time. For enveloped viruses, the viral release is generating cell death by lysis of the producer cells. Consequently, a viability below 90% is observed in **Phase II & III**. In addition to ion efflux, cell shrinkage or cell membrane porosity induced by cell death process are likely to impact σi values (Ansorge et al., 2010b; Labeed et al., 2006). Different reports have already discussed the limits of the Pauly and Schwan model to accurately predict the cell death phases (Patel and Markx, 2008): The mathematical models of Pauly and Schwan describing fc and permittivity signals are applicable only for live cells with intact cell membranes. Consequently, in the present case and for the following viral productions, σi and Cm evolutions will not be discussed when cell viability is below 90%.

Literature studies of intracellular conductivity (σi) reported proportionality of this parameter with intracellular ion concentration (Pilwat and Zimmermann, 1985). Alteration of the cytoplasmic ion content of infected cells has been described for a variety of viruses, and at different stages of their replication cycle (del Castillo et al., 1991; Hackstadt and Mallavia, 1982; Nair, 1984; Palù et al., 1994; Voss et al., 1996). Consequently, we assume that the intracellular accumulation of large amount of reovirus/cell during **Phase I** impacts the infected HEK293 cytoplasmic conductivity.

With regards to membrane capacitance (Cm), this parameter represents the membrane capacity to store electric charges and is thus correlated with membrane area (Cm = C/S). This dielectric characteristic has been related to i) folding of the membrane in microvilli, ii) level of proteins embedded in the membrane or iii) the membrane thickness (Benz et al., 1973; Zimmermann et al., 2008). The rapid increase of HEK293 cell size and its related increase of membrane surface (~10% between 20 and 40 hpi), is generally observed to result in membrane smoothing and microvilli disappearance (Zimmermann et al., 2008).

3.2. Enveloped viruses

Fig. 2 presents the monitoring of four cultures, respectively, A) an influenza virus production, B) a lentivirus production and C & D) two baculoviruses productions performed at different MOIs (0.2 and 2.0). The on-line acquisition of permittivity, $\Delta\varepsilon_{max}$, and characteristic frequency, fc, were plotted with off-line assessed cell concentration, viability, cell size, biovolume and viral titers measured on culture samples. Fig. 3 and Table 4 present the evolutions of the calculated parameters σi and Cm as described in the Material

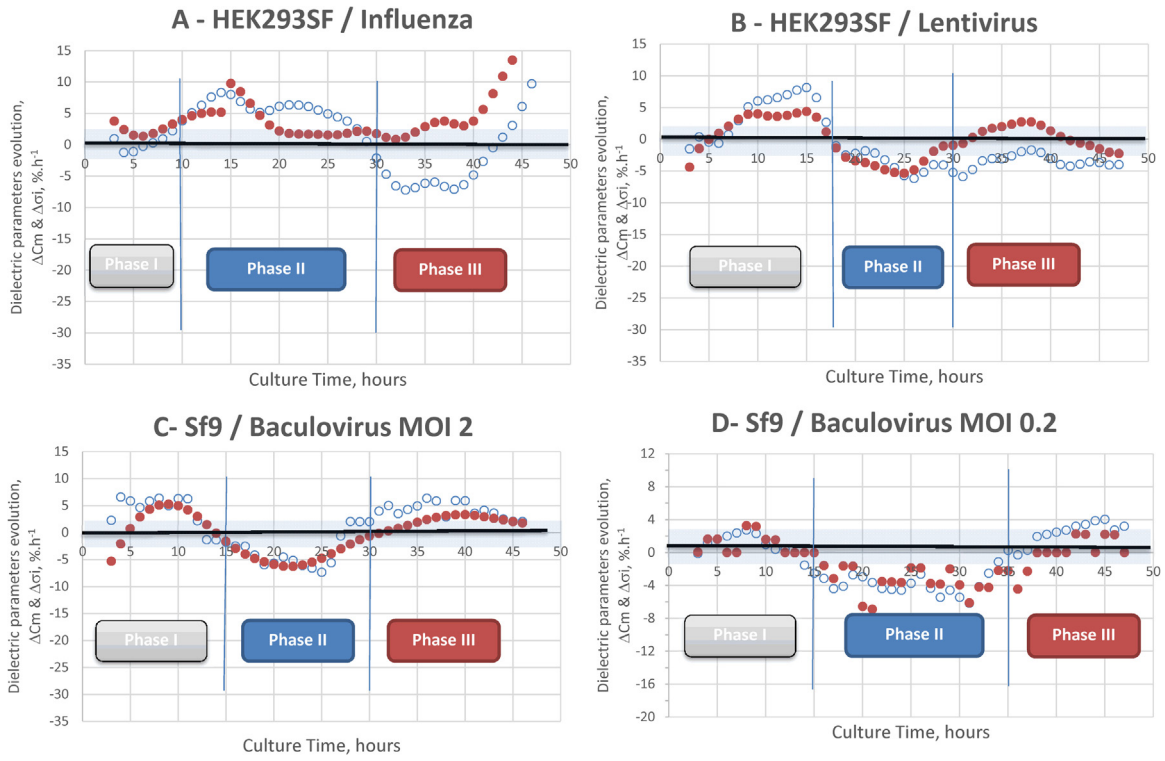

Fig. 4. Percentage of dielectric parameters evolutions per hour (ΔCm (○) & Δσi (●)) over the culture: The percentage of evolution of a parameter (P) calculated per hour as follows: $((P_{t+1}-P_{t-1}).100) \div ((t+1)-(t-1).P_t)$. Blue area represent the significance cut-off of the parameters corresponding at 2% per hour. (For interpretation of the references to colour in this figure legend, the reader is referred to the web version of this article.)

& Methods section. They are presented with the viral titers and the fc signal evolutions for all four cultures described above.

3.2.1. Viral production method (transfection versus infection)

From the cultures presented in this study, lentivirus is the only virus produced by cellular transfection. All the other viruses were produced by direct infection with live viruses.

Lentivirus production during the first hour post-transfection, displayed similar trends for fc and $\Delta\varepsilon_{max}$ signals as the baculovirus or influenza process using direct infection. Indeed, right after infection/transfection (0–5 hpi), the cell population exhibits a V-shape pattern in the fc signal, indicative of the cellular effect of the virus entry process or of the transfectant mediated plasmid DNA entry (indicated as a grey arrow on Fig. 2A-1, B-1). Only in the case of influenza production, a concomitant increase of $\Delta\varepsilon_{max}$ signal is observed. It is important to note that influenza infection process is the only virus necessitating trypsin activation. Trypsin added in the culture broth was already shown to be responsible of such $\Delta\varepsilon_{max}$ signal behaviour (Petiot et al., 2012b). No typical patterns associated specifically with either infection or transfection were identified.

Consequently, based only on such observations, the production mode (infection or transfection) does not directly seem to impact the dielectric properties of a cell population.

3.2.2. Viral assembly localization

Both, the viral structure and its assembly process may strongly affect cellular characteristics during production. In the present case, two enveloped virus types were used. The first group, composed of baculovirus and lentivirus, possesses nucleocapsid that assemble in the cytoplasm, whereas the second group composed of influenza virus does not, but is rather composed of antigenic glycoproteins and matrix proteins M1 & M2 that assemble at the cell membrane. As previously indicated, the $\Delta\varepsilon_{max}$ signal is a good indicator of the biovolume evolution. In the case of baculovirus and lentivirus productions, $\Delta\varepsilon_{max}$ increased significantly by the time the progeny viruses were released (Fig. 2B-2, C-2 & D-2), whereas for influenza virus the $\Delta\varepsilon_{max}$ remained almost constant (Fig. 2A-2). Both baculovirus and lentivirus possess viral capsids that assemble in the cytoplasm before budding and similarly to non-enveloped virus, an accumulation of viral capsid accounts for an increase in cell size and permittivity $\Delta\varepsilon_{max}$ that is measured. Such phenomena have been extensively documented for baculovirus infected cells (Ansorge et al., 2011; Zeiser et al., 2000, 1999). In the present case, the increase in cell size was more pronounced for baculovirus productions than for lentivirus, most probably related to their larger capsids and their shape (rod shape versus circular) as summarized in Table 1 (M&M section) (Acheson, 2007a). On the contrary, influenza viruses assemble directly at the plasma membrane, and during the budding process only a lipid bilayer is acquired from the cell membrane to envelop their genome (Acheson, 2007b). Influenza virus production in HEK293 cells is characterized by a cell diameter reduction, most likely due to a rapid cell death process (Petiot et al., 2011).

3.2.3. Viral production kinetics

3.2.3.1. Effect of multiplicity of infection (MOI) and identification of the timing of the viral release. The multiplicity of infection (MOI) controls the number of infection cycles occurring during the production process, each infection cycle ending with a viral release. Higher MOI than 1.0 viral particle per cell are generally chosen to infect all the cell population simultaneously (synchronous infection). The purpose of using low MOI for viral production is to generate multiple infection cycles in the culture, allowing the cells to grow and to have multiple viral release steps before inducing cell death. In order to observe the impact of viral kinetics on the on-line signals, a high MOI of 2.0 and a low MOI of 0.2 were tested to produce baculoviruses in Sf9 cells (Fig. 2C & D).

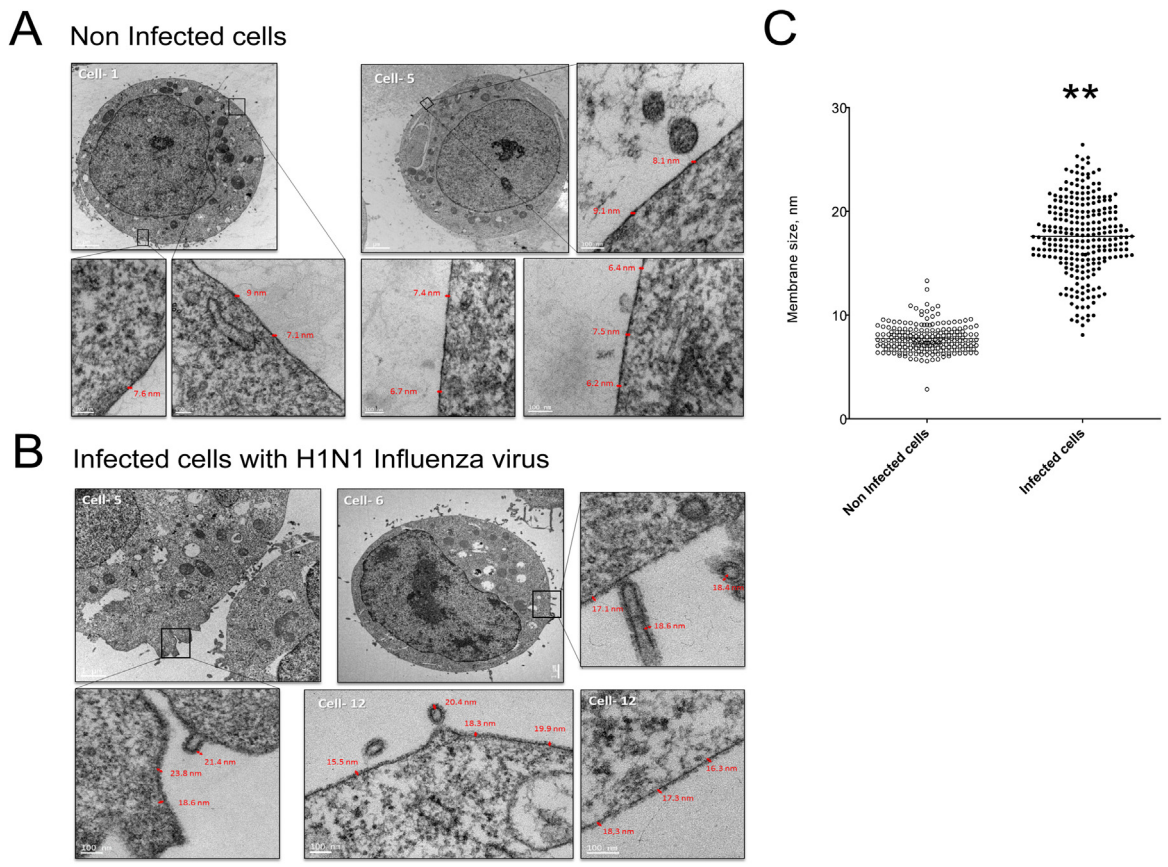

Fig. 5. Membrane size evolution of HEK293 cells under infection by influenza virus. A- Electron microscopy observations and membrane size measurements of non-infected HEK 293 cells at 3×10^6 cell/mL (eq. to 30 h post-infection). B- Electron microscopy observations and membrane size measurements of infected HEK 293 cells with A/Puerto Rico/8/34 H1N1 Influenza at 30 hpi. C- Distribution of membrane cell size measurements for infected and non-infected HEK293 cells. Significance of the difference (p value < 0.05) is indicated by **.

The trends observed in the permittivity signal were consistent with previous observations made for this viral production system. The permittivity ($\Delta\varepsilon_{max}$) increase along the viral production process is driven by the biovolume and the cell size increase. Such observations have already been made for the baculovirus expression system using Sf9 cells (Zeiser et al., 2000; Ansorge et al., 2007; Ansorge et al., 2010a). The maximum values of $\Delta\varepsilon_{max}$ and their timing differ for the two MOI conditions. The low MOI condition has a maximum $\Delta\varepsilon_{max}$ of 25 pF.m^{-1}, which is 70% higher than the value obtained for the high MOI condition. This value is reached at 30 hpi, or approximately 15 h later than the maximum obtained for the high MOI of 2.0. This is consistent with the post-infection cell growth observed in low MOI condition, reaching a cell density of 4.5×10^6 cell/mL at 30 hpi whereas the growth of the high MOI condition was stopped right after infection.

Comparison of the influenza and lentivirus cultures demonstrates that the monitoring of fc signals is relevant in these systems (Fig. 2A-2 & B-2). A similar V-shape profile of fc was observed in all four cultures although the selected three cell-virus production systems differ in their production mode (infection vs transfection), viral shape, viral size or assembly mode. This V-shape profile is indicated on Fig. 2 with blue arrows. This pattern is concomitant with viral release in the four different cultures. This is a very important finding supporting the demonstration that macroscopic capacitance signals allow for an effective monitoring of viral productions kinetics by providing informations on the particle release timing. It is noteworthy that for influenza production in HEK293 cells, as well as for lentivirus production, the amplitude of the fc V-shape pattern has been correlated with cell productivity (Ansorge et al., 2011; Petiot et al., 2012b).

3.2.3.2. Viral cycle stage and cellular dielectric properties. The dielectric properties of the cell population (Cm & σi) were calculated and their evolution were compared with the different viral production phases of the three enveloped viruses. This is presented in Figs. 3 and 4 and Table 4. Similarities and discrepancies in the evolution of Cm and σi parameters during the different viral kinetic production phases are further detailed below.

Phase I, corresponding to the intracellular accumulation of viral components (viral proteins, capsids and genomes), was defined as the phase before the viral release. During this phase and for all the viral productions, both Cm and σi parameters increased with rates ranging from 1 to 5% per hour as indicated in Fig. 4 and Table 4. The viral production phase **(Phase II)**, was identified by the onset of viral particle release. In **Phase II**, discrepancies in the dielectric parameter behaviour were observed between influenza production and the other cell-virus systems. In contrast to influenza production, where Cm and σi continue to increase, lentivirus and baculoviruses production systems were characterized by a decrease in both Cm and σi values (20–30% decrease). After that and similar to infection processes with non-enveloped viruses, the dielectric properties Cm and σi could not be exploited for **Phase III** due to the limitations of the Pauly and Schawn model. Nevertheless, the fc and permittivity profiles were clearly indicative of cell death. The characteristic frequency fc has already been associated with cell death occurrence in previous studies and was used for the monitoring of apopto-

sis onset after nutrient deprivation or drug induction (Petiot et al., 2012a; Zalai et al., 2015). In our case, the strong increase of fc signal associated to a decrease in permittivity measurements was indicative of cell death onset induced by viral production. The increase of fc was observed in parallel to a loss of more than 30% of the viable cells (until harvest) for all the viral productions (Fig. 2).

It is generally difficult to link the evolution of dielectric parameters and the viral replication cycle without direct measures of Cm and σi. However, to complement these observations, in the particular case of influenza virus, Cm and σi evolutions could be interpreted on the basis of knowledges on the influenza replication cycle in HEK293 cells (Petiot et al., 2012b).

Between 1 and 15 hpi, Cm and σi increase is weak (only 50% of its initial value). Recent studies of influenza production kinetics demonstrates that only 10% of the cell population is infected with a MOI of 0.01 during a first viral-cycle lasting 8–12 h (Petiot et al., 2012b). The first viral release provides enough progeny virions to infect 100% of the cell population in a second round of infection. From 10 hpi to 30 hpi, the increase in Cm and σi is greater (more than 150% of its original value), reaching a maximum of 1 μF/Cm^2 and 7.5 mS/Cm. As already reported, membrane capacitance (Cm) is influenced by the membrane composition (embedded proteins/lipids), the membrane folding or the membrane thickness (Gentet et al., 2000; Zimmermann et al., 2008). A high expression rate of transmembrane and underlying viral proteins could lead to a strong modification of the membrane capacitance (Zimmermann et al., 2008). After 30 hpi, all cells are infected and achieve their highest production capacities, and cell membranes are full of influenza matrix proteins M1 and M2 and antigenic glycoproteins HA and NA. In the present case, HEK293 cells were producing approximately 10 000 infectious virions/cell with approximately 500 to 750 glycoproteins per virions (Moulès et al., 2011).

The impact of the influenza viral infection on cell membrane was also confirmed by electron microscopy (EM) measurements of HEK293 cell membrane thickness after 35 hpi (Fig. 5). These EM experiments showed membrane thickness reaching a mean value of 17 nm in infected cells, whereas non-infected cells exhibited a thickness of 8 nm only. Such increase in membrane thickness was already proposed to be responsible of Cm diminution, as observed after 35 hpi (Zimmermann et al., 2008). The effect of infection on membrane folding was also confirmed with the observation of infected cells presenting multiple microvilli unlike non-infected cell membranes.

The increase of σi (≥40% from its original value) during the intracellular production phase (**Phase I & II)** could be, at least partially, explained by an accumulation of viral components inside the cytoplasm before the onset of the viral budding. For lentivirus and baculovirus, accumulation of capsids within the cells has already related to the cell biovolume increase. So, upon infection, concomitant increase of σi and cell size is an additional confirmation of the impact of viral infection progress on the cell and its dielectric properties. σi diminution during viral release would suggest that intracellular content of viral protein/capsids progressively decrease as soon as the budding process starts.

Consequently, Cm and σi evolution during **Phase I** for enveloped virus productions is indicative of an intracellular accumulation of viral proteins and/or capsids. Furthermore, an increased number of viral proteins embedded in the cell membrane affects its thickness, and eventually contribute to increase folding of the cell membrane following viral budding inception. Cm and σi diminution during viral release (**Phase II**) would suggest that cell dielectric properties are reset to their initial state, with the partial release of the intracellular content (viral proteins) and budded virus with a decrease in cell membrane folding. In the case of viral production kinetics with low MOI (influenza and baculovirus 4-D), the onset of **Phase II** is more complex to interpret. Viral release is expected to start as earlier as 8–10 hpi. In the meantime, different cell populations at different stage of infection are undergoing simultaneously viral synthesis, viral release and a secondary infection cycle. It is only after 30 hpi, that all the cells are releasing viruses, time at which the cell death onset is observed.

4. Conclusion

On-line monitoring of capacitance signals is well documented as an excellent marker of the cell physiological state in cell culture processes. Exploiting this technology for different viral production systems demonstrates that it is also a valuable tool to monitor the behaviour of cell cultures following viral infection, and consequently allowing for the monitoring of viral production kinetics. More detailed analyses of the cell dielectric properties showed that the membrane capacitance and the intracellular conductivity were strongly altered during the viral production phase. Differences in cell dielectric properties appear to be specific to the type of virus produced (enveloped/non-enveloped particle, viral size and intracellular location of viral assembly). For each of the enveloped virus production runs that were analyzed, a characteristic pattern of the dielectric parameters ($\Delta\varepsilon_{max,}$ fc) and properties (Cm and σi) was identified. This pattern indicated the onset/ending of critical process phases as the viral release or the cell death. In the case of non-enveloped virus production, changes in cell dielectric parameters due to virus replication were only observable immediately before viral release, corresponding to the time when progeny virions are expelled out of the cells through lysis. Nevertheless, the intracellular accumulation of viral capsid in the cell cytoplasm was associated with typical changes in the parameters Cm and σi; this observation is similar to the observation made during the replication phase of enveloped viruses. Further work focusing on off-line determination of dielectric properties using methods such as electro rotation should help confirming the calculations of the changes in Cm and σi that was presented herein.

By taking advantage of the current state of the art in dielectric spectroscopy measurements, this study demonstrates that the technology has the potential to support in-line monitoring and process supervision of a wide variety of processes in the viral vaccines and viral vectors manufacturing field. This technique should be helpful to better document and supervise batch or perfusion viral production processes, especially the one with transient production phases, as for influenza and lentivirus, presented in this paper. But more importantly, such technology could lead to important advance for viral process control for continuous virus production processes, where the infected-cell status has to be controlled to a predefined set point.

Acknowledgements

The authors would like to thank Christine Thompson, Johnny Montes, Stephane Lanthier, Danielle Jacob, Robert Voyer, Julia Transfiguracion, and Chun Fang Shen for bioreactor operation from which the data were exploited and general support in this project. The authors thank also Elisabeth Errazuriz-Cerda from the Centre d'Imagerie Quantitative Lyon-Est (CIQLE, Université Claude Bernard Lyon 1, Lyon, France) for the electron microscopy sample preparation and observations.

Appendix A. Supplementary data

Supplementary data associated with this article can be found, in the online version, at http://dx.doi.org/10.1016/j.jbiotec.2016.11.010.

References

Acheson, N.h., 2007a. Fundamentals of Molecular Virology, ed. Wiley.

Acheson, N.h., 2007b. Orthomyxoviruses. In: Witt, K. (Ed.), Fundamentals of Molecular Virology. , pp. 248–260.

Al-Rubeai, M., Singh, R.P., 1998. Apoptosis in cell culture. Curr. Biol. 9, 152–156.

Ansorge, S., Esteban, G., Schmid, G., 2007. On-line monitoring of infected Sf-9 insect cell cultures by scanning permittivity measurements and comparison with off-line biovolume measurements. Cytotechnology 55, 115–124, http://dx.doi.org/10.1007/s10616-007-9093-0.

Ansorge, S., Lanthier, S., Transfiguracion, J., Durocher, Y., Henry, O., Kamen, A., 2009. Development of a scalable process for high-yield lentiviral vector production by transient transfection of HEK293 suspension cultures. J. Gene Med. 11, 868–876.

Ansorge, S., Esteban, G., Schmid, G., 2010a. On-line monitoring of responses to nutrient feed additions by multi-frequency permittivity measurements in fed-batch cultivations of CHO cells. Cytotechnology 62, 121–132, http://dx.doi.org/10.1007/s10616-010-9267-z.

Ansorge, S., Esteban, G., Schmid, G., 2010b. Multifrequency permittivity measurements enable on-line monitoring of changes in intracellular conductivity due to nutrient limitations during batch cultivations of CHO cells. Biotechnol. Prog. 26, 272–283, http://dx.doi.org/10.1002/btpr.347.

Ansorge, S., Henry, O., Aucoin, M., Voyer, R., Carvell, J.P., Kamen, A.A., 2010c. on-line monitoring of cell size distribution in mammalian cell culture processes. In: Noll, T. (Ed.), Cells and Culture: Proceedings of the 20th ESACT Meeting, Dresden, Germany. Springer Netherlands, Dordrecht, pp. 853–859, http://dx.doi.org/10.1007/978-90-481-3419-9_150.

Ansorge, S., Henry, O., Kamen, A., 2010d. Recent progress in lentiviral vector mass production. Biochem. Eng. J. 48, 362–377.

Ansorge, S., Lanthier, S., Transfiguracion, J., Henry, O., Kamen, A., 2011. Monitoring lentiviral vector production kinetics using online permittivity measurements. Biochem. Eng. J. 54, 16–25, http://dx.doi.org/10.1016/j.bej.2011.01.002.

Archer, S., Morgan, H., Rixon, F.J., 1999. Electrorotation studies of baby hamster kidney fibroblasts infected with herpes simplex virus type 1. Biophys. J. 76, 2833.

Arnold, W.M., Zimmermann, U., 1988. Electro-rotation: development of a technique for dielectric measurements on individual cells and particles. J. Electrostat. 21, 151–191.

Aucoin, M.G., Jacob, D., Chahal, P.S., Meghrous, J., Bernier, A., Kamen, A.A., 2007. Virus-like particle and viral vector production using the baculovirus expression vector system/insect cell system: adeno-associated virus-based products. Methods Mol. Biol. 388, 281–296.

Benz, R., Stark, G., Janko, K., Läuger, P., 1973. Valinomycin-mediated ion transport through neutral lipid membranes: influence of hydrocarbon chain length and temperature. J. Membr. Biol. 14, 339–364.

Bernal, V., Carinhas, N., Yokomizo, A.Y., Carrondo, M.J.T., Alves, P.M., 2009. Cell density effect in the baculovirus-insect cells system: a quantitative analysis of energetic metabolism. Biotechnol. Bioeng. 104, 162–180, http://dx.doi.org/10.1002/bit.22364.

Bronzino, E.J.D., Roth, B.J., 2000. Roth, B. J. The Electrical Conductivity of Tissues. Biochem. Eng. Handb. Second Ed.

Brun, A., Albina, E., Barret, T., Chapman, D.A.G., Czub, M., Dixon, L.K., Keil, G.M., Klonjkowski, B., Le Potier, M.-F., Libeau, G., Ortego, J., Richardson, J., Takamatsu, H.-H., 2008. Antigen delivery systems for veterinary vaccine development: viral-vector based delivery systems. Vaccine 26, 6508–6528.

Buonagurio, D.A., Neill, R.E.O., Shutyak, L., Arco, G.A.D., Bechert, T.M., Kazachkov, Y., Wang, H., Destefano, J., Coelingh, K.L., August, M., Parks, C.L., Zamb, T.J., Sidhu, M.S., Udem, S.A., 2006. Genetic and phenotypic stability of cold-adapted influenza viruses in a trivalent vaccine administered to children in a day care setting 347, 296–306. 10.1016/j.virol.2005.11.006.

Côté, J., Garnier, A., Massie, B., Kamen, A., Cote, J., 1998. Serum-free production of recombinant proteins and adenoviral vectors by 293SF-3F6 cells. Biotechnol. Bioeng. 59, 567–575.

Costin, J.M., 2007. Cytopathic mechanisms of HIV-1. Virol. J. 4, 100, http://dx.doi.org/10.1186/1743-422X-4-100.

Draper, S.J., Heeney, J.L., 2010. Viruses as vaccine vectors for infectious diseases and cancer. Nat. Rev. Microbiol. 8, 62–73, http://dx.doi.org/10.1038/nrmicro2240.

Ducommun, P., Kadouri, A., von Stockar, U., Marison, I.W., 2002. On-line determination of animal cell concentration in two industrial high-density culture processes by dielectric spectroscopy. Biotechnol. Bioeng. 77, 316–323.

Durocher, Y., Pham, P.L., St-Laurent, G., Jacob, D., Cass, B., Chahal, P., Lau, C.J., Nalbantoglu, J., Kamen, A., 2007. Scalable serum-free production of recombinant adeno-associated virus type 2 by transfection of 293 suspension cells. J. Virol. Methods 144, 32–40.

Elias, C.B., Zeiser, A., Bedard, C., Kamen, A.A., Voyer, R., Jardin, B., Tom, R., 2000. Enhanced growth of Sf-9 cells to a maximum density of 5.2 × 10(7) cells per mL and production of beta-galactosidase at high cell density by fed batch culture. Biotechnol. Bioeng. 68, 381–388.

FDA, 2004. Guidance for Industry Guidance for Industry PAT—A Framework for Innovative Pharmaceutical, Development, Manufacturing, and Quality Assurance, Quality Assurance. FDA.

Genet, L.J., Stuart, G.J., Clements, J.D., 2000. Direct measurement of specific membrane capacitance in neurons. Biophys. J. 79, 314–320, http://dx.doi.org/10.1016/s0006-3495(00)76293-x.

Gentet, L.J., Stuart, G.J., Clements, J.D., 2000. Direct measurement of specific membrane capacitance in neurons. Biophys. J. 79, 314–320, http://dx.doi.org/10.1016/S0006-3495(00)76293-X.

Ghani, K., Garnier, A., Coelho, H., Transfiguracion, J., Trudel, P., Kamen, A., 2006. Retroviral vector production using suspension-adapted 293GPG cells in a 3L acoustic filter-based perfusion bioreactor. Biotechnol. Bioeng. 95, 653–660.

Hackstadt, T., Mallavia, L.P., 1982. Sodium and potassium transport in herpes simplex virus-infected cells. J. Gen. Virol. 60, 199–207.

Haupt, R.M., Sings, H.L., 2011. The efficacy and safety of the quadrivalent human papillomavirus 6/11/16/18 vaccine gardasil. J. Adolesc. Health 49, 467–475, http://dx.doi.org/10.1016/j.jadohealth.2011.07.003.

Hinshaw, V.S., Olsen, C.W., Dybdahl-Sissoko, N., Evans, D., 1994. Apoptosis: a mechanism of cell killing by influenza A and B viruses. J. Virol. 68, 3667–3673.

Hopkins, R., Esposito, D., 2009. A rapid method for titrating baculovirus stocks using the Sf-9 Easy Titer cell line. Biotechniques 47, 785–788, http://dx.doi.org/10.2144/000113238.

Josset, L., Frobert, E., Rosa-Calatrava, M., 2008. Influenza A replication and host nuclear compartments: many changes and many questions. J. Clin. Virol. 4, 381–390.

Kamen, A., Henry, O., 2004. Development and optimization of an adenovirus production process. J. Gene Med. 6 (Suppl. 1), S184–S192.

Knop, D.R., Harrell, H., 2007. Bioreactor production of recombinant herpes simplex virus vectors. Biotechnol. Prog.

Labeed, F.H., Coley, H.M., Hughes, M.P., 2006. Differences in the biophysical properties of membrane and cytoplasm of apoptotic cells revealed using dielectrophoresis. Biochim. Biophys. Acta Gen. Subj. 1760, 922–929, http://dx.doi.org/10.1016/j.bbagen.2006.01.018.

Le Ru, A., Jacob, D., Transfiguracion, J., Ansorge, S., Henry, O., Kamen, A.A., 2010. Scalable production of influenza virus in HEK-293 cells for efficient vaccine manufacturing. Vaccine 28, 3661–3671, http://dx.doi.org/10.1016/j.vaccine.2010.03.029.

Lentz, T.B., Gray, S.J., Samulski, R.J., 2011. Viral vectors for gene delivery to the central nervous system. Neurobiol. Dis. 8, 21–34, http://dx.doi.org/10.1016/j.nbd.2011.09.014.

Meghrous, J., Aucoin, M.G., Jacob, D., Chahal, P.S., Arcand, N., Kamen, A.A., 2005. Production of recombinant adeno-associated viral vectors using a baculovirus/insect cell suspension culture system: from shake flasks to a 20-L bioreactor. Biotechnol. Prog. 21, 154–160.

Moulès, V., Terrier, O., Yver, M., Riteau, B., Moriscot, C., Ferraris, O., Julien, T., Giudice, E., Rolland, J.-P., Erny, A., Bouscambert-Duchamp, M., Frobert, E., Rosa-Calatrava, M., Pu Lin, Y., Hay, A., Thomas, D., Schoehn, G., Lina, B., 2011. Importance of viral genomic composition in modulating glycoprotein content on the surface of influenza virus particles. Virology 414, 51–62, http://dx.doi.org/10.1016/j.virol.2011.03.011.

Nair, C.N., 1984. Na and K changes in animal virus-infected HeLa cells. J. Gen. Virol. 65 (Pt 6), 1135–1138.

Noll, T., Biselli, M., 1998. Dielectric spectroscopy in the cultivation of suspended and immobilized hybridoma cells. J. Biotechnol. 63, 187–198.

Opel, C.F., Li, J., Amanullah, A., 2010. Quantitative modeling of viable cell density, cell size, intracellular conductivity, and membrane capacitance in batch and fed-batch CHO processes using dielectric spectroscopy. Biotechnol. Prog. 26, 1187–1199, http://dx.doi.org/10.1002/btpr.425.

Párta, L., Zalai, D., Borbély, S., Putics, Á., 2013. Application of dielectric spectroscopy for monitoring high cell density in monoclonal antibody producing CHO cell cultivations. Bioprocess Biosyst. Eng. 37, 311–323, http://dx.doi.org/10.1007/s00449-013-0998-z.

Paillet, C., Forno, G., Kratje, R., Etcheverrigaray, M., 2009. Suspension-Vero cell cultures as a platform for viral vaccine production. Vaccine 27, 6464–6467, http://dx.doi.org/10.1016/j.vaccine.2009.06.020.

Palù, G., Biasolo, M., a Sartor, G., Masotti, L., Papini, E., Floreani, M., Palatini, P., 1994. Effects of herpes simplex virus type 1 infection on the plasma membrane and related functions of HeLa S3 cells. J. Gen. Virol. 75 (Pt. 12), 3337–3344.

Palomares, L., Pedroza, J., Ramirez, O., 2001. Cell size as a tool to predict the production of recombinant protein by the insect-cell baculovirus expression system. Biotechnol. Lett. 23, 359.

Patel, P.M., Markx, G.H., 2008. Dielectric measurement of cell death. Enzyme Microb. Technol. 43, 463–470, http://dx.doi.org/10.1016/j.enzmictec.2008.09.005.

Pau, M.G., Ophorst, C., Koldijk, M.H., Schouten, G., Mehtali, M., Uytdehaag, F., 2001. The human cell line PER.C6 provides a new manufacturing system for the production of influenza vaccines. Vaccine 19, 2716–2721.

Pauly, H., Packer, L., 1960. The relationship of internal conductance and membrane capacity to mitochondrial volume. J. Biophys. Biochem. Cytol. 7, 603–612.

Petiot, E., Jacob, D., Lanthier, S., Lohr, V., Ansorge, S., Kamen, A.A., 2011. Metabolic and kinetic analyses of influenza production in perfusion HEK293 cell culture. BMC Biotechnol. 11, 84, 1472-6750-11-84 [pii]10.1186/1472-6750-11-84.

Petiot, E., El-Wajgali, A., Esteban, G., Gény, C., Pinton, H., Marc, A., 2012a. Real-time monitoring of adherent vero cell density and apoptosis in bioreactor processes. Cytotechnology, http://dx.doi.org/10.1007/s10616-011-9421-2.

Petiot, E., Kamen, A.A., Emma, P., 2012b. Real-time monitoring of influenza virus production kinetics in HEK293 cell cultures. Biotechnol. Prog., http://dx.doi.org/10.1002/btpr.1601.

Pilwat, G., Zimmermann, U., 1985. Determination of intracellular conductivity from electrical breakdown measurements. Biochim. Biophys. Acta 820, 305–314.

Schwan, H.P., 1957. Electrical properties of tissue and cell suspensions. Adv. Biol. Med. Phys. 5, 147–208.

Segura, M.D.L.M., Garnier, A., Kamen, A., 2006. Purification and characterization of retrovirus vector particles by rate zonal ultracentrifugation. J. Virol. Methods 133, 82–91.

Stinstra, J.G., Hopenfeld, B., Macleod, R.S., 2005. On the passive cardiac conductivity. Ann. Biomed. Eng. 33, 1743–1751, http://dx.doi.org/10.1007/s10439-005-7257-7.

Terrier, O., Moules, V., Carron, C., Cartet, G., Frobert, E., Yver, M., Traversier, A., Wolff, T., Riteau, B., Naffakh, N., Lina, B., Diaz, J.-J., Rosa-Calatrava, M., 2012. The influenza fingerprints: NS1 and M1 proteins contribute to specific host cell ultrastructure signatures upon infection by different influenza A viruses. Virology 432, 204–218, http://dx.doi.org/10.1016/j.virol.2012.05.019.

Tibayrenc, P., Preziosi-Belloy, L., Ghommidh, C., 2011. On-line monitoring of dielectrical properties of yeast cells during a stress-model alcoholic fermentation. Process Biochem. 46, 193–201, http://dx.doi.org/10.1016/j.procbio.2010.08.007.

Van Gessel, Y., Klade, C.S., Putnak, R., Formica, A., Krasaesub, S., Spruth, M., Cena, B., Tungtaeng, A., Gettayacamin, M., Dewasthaly, S., 2011. Correlation of protection against Japanese encephalitis virus and JE vaccine (IXIARO(®)) induced neutralizing antibody titers. Vaccine 29, 5925–5931, http://dx.doi.org/10.1016/j.vaccine.2011.06.062.

Voss, T.G., Fermin, C.D., Levy, J., a Vigh, S., Choi, B., Garry, R.F., 1996. Alteration of intracellular potassium and sodium concentrations correlates with induction of cytopathic effects by human immunodeficiency virus. J. Virol. 70, 5447–5454.

Whitford, W., Fairbank, A., 2011. Considerations in scale-up of viral vaccine production. Bioprocess Int. 9, 15–28.

Wong, T.K., Nielsen, L.K., Greenfield, P.F., Reid, S., 1994. Relationship between oxygen uptake rate and time of infection of Sf9 insect cells infected with a recombinant baculovirus. Cytotechnology 15, 157–167.

Zalai, D., Tobak, T., Putics, A., 2015. Impact of apoptosis on the on-line measured dielectric properties of CHO cells. Bioprocess Biosyst. Eng., 2427–2437, Doi: 10.1007/s00449-015-1479-3.

Zeiser, A., Bédard, C., Voyer, R., Jardin, B., Tom, R., Kamen, A.A., 1999. On-line monitoring of the progress of infection in Sf-9 insect cell cultures using relative permittivity measurements. Biotechnol. Bioeng. 63, 122–126.

Zeiser, A., Elias, C.B., Voyer, R., Jardin, B., Kamen, A.A., 2000. On-line monitoring of physiological parameters of insect cell cultures during the growth and infection process. Biotechnol. Prog. 16, 803–808.

Zimmermann, D., Terpitz, U., Zhou, A., Reuss, R., Müller, K., Sukhorukov, V.L., Gessner, P., Nagel, G., Zimmermann, U., Bamberg, E., 2006. Biophysical characterisation of electrofused giant HEK293-cells as a novel electrophysiological expression system. Biochem. Biophys. Res. Commun. 348, 673–681.

Zimmermann, D., Zhou, A., Kiesel, M., Feldbauer, K., Terpitz, U., Haase, W., Schneider-Hohendorf, T., Bamberg, E., Sukhorukov, V.L., 2008. Effects on capacitance by overexpression of membrane proteins. Biochem. Biophys. Res. Commun. 369, 1022–1026, http://dx.doi.org/10.1016/j.bbrc.2008.02.153.

del Castillo, J.R., Ludert, J.E., Sanchez a Ruiz, M.C., Michelangeli, F., Liprandi, F., 1991. Rotavirus infection alters Na+ and K+ homeostasis in MA-104 cells. J. Gen. Virol. 72 (Pt. 3), 541–547.